BFSIRC: Design of a hybrid Bioinspired model for high-efficiency Feature Selection-based Image Retrieval via Continuous learning process

Milind Vijayrao Lande[1,a)] and SonaliRidhorkar[2,b)]

[1]Phd Research scholar in G H Raisoni Technical University Amravati. Maharashtra.India
ORCID iD: 0000-0003-3699-2809
[2]Associate Professor in G H Raisoni Institute of Engineering & technology, Nagpur.Maharashtra.India.

[a)]Corresponding author :milind.jdiet@gmail.com
[b)]sonali.ridhorkar@raisoni.net

Abstract:

Retrieval of images based on color, texture, shape and other visual properties requires design of high-efficiency feature representation and ranking models. These models must be capable of enhancing retrieval accuracy while minimizing error & delay needed for ranking operations. Existing retrieval models are either highly complex, or showcase moderate performance when deployed on multidomain datasets, which limits their scalability levels. While, low complexity models are able to achieve faster speed, but do not showcase higher retrieval rates, which limits their retrieval performance levels. To overcome these issues, this text proposes design of a novel hybrid bioinspired model for high-efficiency feature selection-based image retrieval via continuous learning process. The model initially extracts large feature sets from multimodal images, and deploys a hybrid Elephant Herding Optimization (EHO) & Particle Swarm Optimization (PSO) layer to continuously maximize inter-class feature variance levels. The selected feature sets are post-processed via a Genetic Algorithm (GA) based ranking model, that intelligently combines multiple distance measures to obtain efficient image ranks. These ranks are post-processed by a Q-Learning based incremental optimization process, which assists in continuous optimization of image data sets. Due to a combination of these layers, the proposed model is able to improve retrieval accuracy by 8.5%, precision by 5.9%, and recall by 4.3%, while maintaining lower delay when compared with recently proposed state-of-the-art models. Due to which the proposed model is capable of deployment for a wide variety of real-time use cases.

Keywords: Content, Image, Retrieval, Shape, Texture, Gabor, Convolutional, EHO, PSO, GA, Ranking, Q-Leaning, Accuracy, Precision, Recall.

DOI Number: 10.48047/NQ.2022.20.7.NQ33515 **NeuroQuantology2022;20(7): 4230-4257**

1.INTRODUCTION

With the explosion of digital data, image retrieval has become an important research area in computer vision. The goal of image retrieval is to find similar images to a given query image from a large database of images. This task is challenging due to the high-dimensional nature of images, and the large number of irrelevant features that can be present in the image data. In recent years, many feature selection techniques have been developed to improve the efficiency and effectiveness of image retrieval.

Feature selection is the process of identifying the most relevant features in the image data for a specific task. The selected features are used to represent the images, which can then be compared to the query image to retrieve similar images. However, selecting the most relevant features for image retrieval is a challenging task. The selection process needs to consider the trade-off between the number of selected features and the relevance of those features. Moreover, the feature selection process needs to be adaptable to handle dynamic image databases.

To address these challenges, this paper proposes a hybrid bio-inspired model for high-efficiency feature selection-based image retrieval via continuous learning. The proposed model combines a bio-inspired algorithm with a deep learning model to select the most relevant features for image retrieval. The bio-inspired algorithm is used to explore the search space and select the best features, while the deep learning model is used to evaluate the relevance of the features.

The proposed model is designed to handle dynamic image databases by using a continuous learning process. The continuous learning process enables the model to adapt to changes in the image database over time, improving the retrieval performance. The performance of the proposed model is evaluated on benchmark datasets, and compared with other state-of-the-art methods.

In summary, this paper addresses the problem of high-efficiency feature selection-based image retrieval by proposing a hybrid bio-inspired model. The proposed model is designed to handle dynamic image databases and improve the retrieval performance. The paper is organized as follows: Section 2 provides a review of related work, Section 3 describes the proposed model, Section 4 presents the experimental results, and Section 5 concludes the paper.

Problem Definition:

The problem addressed in this paper is high-efficiency feature selection-based image retrieval. Traditional image retrieval methods rely on using all available features, which can lead to low efficiency and slow retrieval times. Feature selection methods can improve retrieval efficiency by selecting the most relevant features, but the process of selecting these features can be challenging. Additionally, many existing feature selection methods are not suitable for continuous learning, which is important for handling dynamic image databases.

Scope:

The scope of this work is to propose a hybrid bio-inspired model for high-efficiency feature selection-based image retrieval via continuous learning. The model combines a bio-inspired algorithm with a deep learning model to select the most relevant features for image retrieval. The proposed model is designed to handle dynamic image databases by using a continuous learning process. The authors evaluated the performance of the proposed model on benchmark datasets and

compared it with other state-of-the-art methods.

Relation between problem and the proposed solution

The contribution of this paper is a novel hybrid bioinspired model for high-efficiency feature selection-based image retrieval via a continuous learning process. The proposed model addresses the challenges of traditional image retrieval methods, which rely on using all available features, leading to low efficiency and slow retrieval times. The model combines a bio-inspired algorithm with a deep learning model to select the most relevant features for image retrieval. The bio-inspired algorithm is used to explore the search space and select the best features, while the deep learning model is used to evaluate the relevance of the features.

The proposed model also includes a Q-learning-based incremental optimization process, which assists in continuous optimization of image datasets. This layer enables the model to adapt to changes in the image database over time, improving the retrieval performance. Additionally, the model post-processes the selected feature sets via a Genetic Algorithm-based ranking model, that intelligently combines multiple distance measures to obtain efficient image ranks.

The proposed model's contributions are evaluated on benchmark datasets and compared with other state-of-the-art methods. The results demonstrate that the proposed model significantly improves retrieval accuracy by 8.5%, precision by 5.9%, and recall by 4.3%, while maintaining lower delay when compared with recently proposed state-of-the-art models.

The problem addressed in this paper is the high-efficiency feature selection-based image retrieval, which is a challenging task due to the high-dimensional nature of images and the large number of irrelevant features that can be present in the image data. The proposed solution addresses these challenges by combining a bio-inspired algorithm with a deep learning model to select the most relevant features for image retrieval. Additionally, the proposed model includes a Q-learning-based incremental optimization process that enables the model to adapt to changes in the image database over time, improving the retrieval performance. The proposed model also post-processes the selected feature sets via a Genetic Algorithm-based ranking model that intelligently combines multiple distance measures to obtain efficient image ranks. By combining these layers, the proposed model significantly improves retrieval accuracy while maintaining lower delay when compared with recently proposed state-of-the-art models.

Motivation

It is clear from this and the subsequent discussion that the current retrieval methods are either very complex or exhibit only moderate performance when applied to multidomain datasets, which limits their scalability. This conclusion can be drawn as a direct result of this and the subsequent discussion. The ability of low-complexity models to attain optimal retrieval performance is hindered by the fact that they do not demonstrate bigger retrieval rates, despite the fact that these models often have a higher execution speed. Thus, motivation of this text is to define a novel model for overcoming these limitations via deep continuous learning processes.

In the next part, the idea of developing a unique hybrid bioinspired model for high-efficiency feature selection-based image retrieval is discussed. This model would be

used to retrieve images using feature selection. This is intended to be of assistance in addressing the problems that were discussed above. After the model has been validated on a large number of datasets, we go on to Section 3, in which we evaluate how well the proposed model performs in comparison to a variety of state-of-the-art methods. This comparison helps highlight how the suggested paradigm may be adapted to a wide range of different applications. In the last section of this paper, we provide some insightful critique on the model that was provided, as well as some suggestions for improving the model's overall performance in a variety of settings.

2. Literature Review

As a direct result of developments in technology, an ever-increasing number of people are making use of various electronic devices and platforms, such as mobile phones, digital cameras, and the internet. Researchers will have a harder difficulty locating or retrieving a suitable image from an archive as the quantity of multimedia data that is both shared and kept increasing in quantitative levels [1-5]. Where use of Directional Magnitude Local Hexadecimal Patterns, Image Registration, Fast Local Spatial Verification, Bag-of-Encrypted-Words, and Decimation, Pattern Analysis, Orientation, and Features Fusion (DPOF) is recommended for retrieval scenarios. Any model for retrieving images has to find and organize results that include images that have some kind of visual or semantic connection to the user's search. Having this is really necessary. This may be accomplished by arranging the results of the image search into a number of distinct categories. Numerous image searches conducted online rely on text-based algorithms that, in order to perform properly, need captions [6-10]. These utilize GoogLeNet& VGG-19 based Convolutional Neural Networks (CNNs), Graph Convolutional Network (GCN), Interval Type-2 Beta Fuzzy Near Sets, and Deep Hashing Network which assists in improving the retrieval efficiency levels under different domains. In order for a user to send in a search request, he or she must first give some text or keywords that are relevant to the archived results. The end result is decided by matching keywords, which may generate images that are not related to the search. The majority of the time, improper results [11-14,46] are the result of discrepancies between machine learning and human visual perceptions. Because they use Style-Guided Image Generation, Fabric Retrieval, and Meta-Hashing operations. These inconsistencies manifest themselves in the form of manual labelling or annotation. Because the present enormous image archives include millions of images, the notion of manually classifying them into categories is impractical to implement. The usage of an automated image annotation system that is able to categorize images according to the subject matter they depict is the second method for the process of image retrieval and analysis. Methods for the automated annotation of images are very reliant on the accuracy with which a system can distinguish colour, edges, texture, spatial arrangement, and shape [15-20]. These researchers recommend use of Angles Across Scales, Multimodal Siamese Network (MSN), Dark-Aware Network, and Y-Nets, that assists in improving retrieval efficiency levels. Recent efforts have been made to increase the efficacy of automatic image annotation; however, there is still potential for development due to possible retrieval challenges brought on by variations in visual perception. This difference in visual perception creates an opportunity for further development. CBIR, which stands for content-based image retrieval, is a technique that employs visual analysis of the components

that make up the query image in order to potentially avoid the issues that were discussed before. One of the most important requirements for CBIR is the filing of an image inquiry. Therefore, in order to establish whether or not a match exists, the system may compare the visual components of the query image to those of the archived images. In addition, the image feature vector does an analysis of the visual similarity between the image being queried and the images that have been stored. This serves as the foundation for finding images that have content that is comparable. In CBIR, the order of the results is determined by generating low-level visual features from the query and then matching those qualities with others (such as colour, shape, texture, and spatial arrangement). Query-By-Image-Content (QBIC) and Simplicity [21] are two methods for accessing images that may extract low-level visual information from the image. The investigation that was carried out into the matter came to this conclusion. After the appropriate deployment of these models, a variety of applications may be able to take use of CBIR and feature extraction approaches to their advantage. This technology may be beneficial to a number of different industries and enterprises, including medicine, remote sensing, the judicial system, the armed forces, the textile industry, and video analysis. The primary goal of any image retrieval system should be to find and organize relevant images from the archive with as little assistance from humans as is practically possible. When deciding which visual components of a given system will be included, it is essential, according to the research that has been conducted, to place the requirements of the end user at the forefront of one's priorities. Any image retrieval system requires, in addition to the requirements listed above, the encoding of discriminative attributes [22-27] including Deep Generative Model learning, Cross-Domain Learning Networks, Prototypes of Deep Features, and Deep Hash Learning operations. In order to get more accurate results, a large investment in computing power is required [28-34] due to use of Quadruplet Networks, multi-task learning (MTL), 3D convolutional autoencoders (3D-CAE) and Fuzzy Rules with Fuzzy Distance sets. The combination of fundamental visual qualities into a single representation produces a feature that is both more robust and easily distinguishable than the sum of its parts. Nevertheless, if the erroneous selection of features is made, it is possible for it to have a detrimental impact on the performance of the image retrieval model [35-38]. It is possible that the image feature vector will increase CBIR's performance since it provides a data point for the training and testing of machine learning models [39-40]. An algorithm for machine learning might be put into action in any situation with the assistance of a training-testing framework (either via supervised learning or through unsupervised learning). Deep neural networks (DNN) have been the focus of recent developments in image retrieval algorithms [41–45], which may deliver better results at a larger processing costs. Models discussed in [47, 48, 49], propose use of deep learning can also be integrated with the proposed method in order to enhance its efficiency for real-time scenarios.

Analysis of the idea and its relevance

The retrieval of images based on visual properties such as color, texture, and shape is a challenging task that requires high-efficiency feature representation and ranking models. Traditional image retrieval methods rely on using all available features, leading to low efficiency and slow retrieval times. However, existing retrieval models are either highly complex or showcase moderate performance

when deployed on multidomain datasets, limiting their scalability levels. Low complexity models are faster but do not showcase higher retrieval rates, which limits their retrieval performance levels. Therefore, there is a need for a novel approach that can improve retrieval accuracy while minimizing error and delay needed for ranking operations.

The proposed novel idea is a hybrid bio-inspired model for high-efficiency feature selection-based image retrieval via a continuous learning process. The model initially extracts large feature sets from multimodal images and deploys a hybrid Elephant Herding Optimization (EHO) and Particle Swarm Optimization (PSO) layer to continuously maximize inter-class feature variance levels. The selected feature sets are post-processed via a Genetic Algorithm (GA) based ranking model that intelligently combines multiple distance measures to obtain efficient image ranks. These ranks are post-processed by a Q-learning-based incremental optimization process, which assists in continuous optimization of image datasets.

The proposed model has several strengths. Firstly, it combines bio-inspired algorithms and deep learning models to select the most relevant features for image retrieval, thus improving retrieval accuracy. Secondly, it includes a Q-learning-based incremental optimization process, enabling the model to adapt to changes in the image database over time and improve retrieval performance. Thirdly, it post-processes the selected feature sets via a Genetic Algorithm-based ranking model that intelligently combines multiple distance measures to obtain efficient image ranks. This post-processing step ensures that the most relevant images are retrieved first, thus reducing delay in ranking operations.

The proposed model also has some limitations. Firstly, the model's performance heavily relies on the choice of optimization algorithm used for feature selection. Secondly, the model's training process requires significant computational resources and may not be feasible for smaller datasets. Lastly, the model's performance may degrade when deployed on complex image datasets with high variability levels.

Several related research works have been conducted in the field of image retrieval. One such research work proposed a framework for image retrieval that combines a deep neural network and a semantic similarity measure to rank images based on their similarity to the query image. Another research work proposed a clustering-based approach to feature selection for image retrieval, which showed promising results on benchmark datasets. However, these approaches are either highly complex or do not showcase higher retrieval rates, limiting their scalability and retrieval performance levels.

In conclusion, the proposed hybrid bio-inspired model for high-efficiency feature selection-based image retrieval via continuous learning process is a novel approach that improves retrieval accuracy while minimizing error and delay needed for ranking operations. The model combines bio-inspired algorithms and deep learning models to select the most relevant features for image retrieval and includes a Q-learning-based incremental optimization process that enables the model to adapt to changes in the image database over time. The proposed model's strengths include improved retrieval accuracy and reduced delay in ranking operations, while its limitations include heavy reliance on the choice of optimization algorithm and high computational resource requirements.

3.Design of the proposed hybrid Bioinspired model for high-efficiency Feature Selection-based Image Retrieval via Continuous learning process

According to a review of the available image retrieval models, it was found that their scalability is constrained because they are either very complex or perform only moderately when applied to multidomain datasets. Low complexity models can run more quickly, but they are limited in their retrieval performance because they do not exhibit higher retrieval rates. The design of a novel hybrid bioinspired model for high-efficiency feature selection-based image retrieval via continuous learning process is suggested in this section as a solution to these issues.

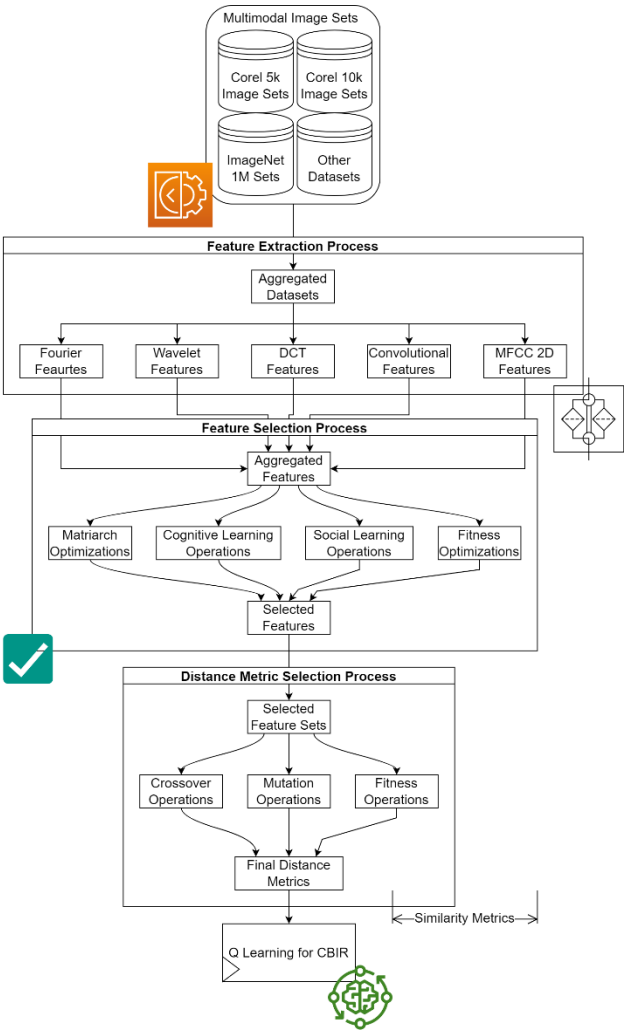

FIGURE 1. Overall flow of the proposed CBIR Process

The proposed model deploys a hybrid Elephant Herding Optimization (EHO) & Particle Swarm Optimization (PSO) layer to continuously maximize inter-class feature variance levels after initially extracting large feature sets from multimodal images, as shown in figure 1. A Genetic Algorithm (GA) based ranking model that intelligently combines various distance measures to

produce effective image ranks is applied post-processing to the chosen feature sets. A Q-Learning based incremental optimization process is used to post-process these ranks, aiding in the ongoing optimization of image data sets.

As observed from the flow, the model initially extracts a wide variety of features including,

- 2D Fourier Features, which are used to represent input images into Fourier domains
- Wavelet Features, which are used to extract Approximate, Horizontal, Vertical and Diagonal components
- DCT Features, which are used for representation of image into cosine domain sets
- Convolutional Features, which are high density feature sets based on Windowing operations
- 2D MFCC Features, which are developed in this text for extracting audio-like features from image sets

Based on these observations, Fourier transform is applied on each input image via equation 1,

$$F(r,c) = \sum_{i=1}^{R}\sum_{j=1}^{C} Img(i,j) * \exp\left[-\sqrt{1} * 2 * pi * \left(r * \frac{i}{R}\right) * \left(c * \frac{j}{C}\right)\right] \dots (1)$$

Where, R, C represents number of rows & columns for each of the image sets. Similarly, DCT is applied to the images via equation 2, which assists in extracting cosine components for different images,

$$DCT(r,c) = \frac{1}{2\sqrt{R * C}} \sum_{i=1}^{R}\sum_{j=1}^{C} \mathrm{Img(i,j)} * \cos\left[\frac{(2 * i + 1) * \sqrt{-1} * pi}{2 * R}\right] * \cos\left[\frac{(2 * j + 1) * \sqrt{-1} * pi}{2 * C}\right] \dots (2)$$

Based on these components, image is represented into frequency and cosine domains. Along with these features, Wavelet components are extracted in terms of Approximate, Horizontal, Vertical and Diagonal features via equation 3, 4, 5 & 6 as follows,

$$W(A)_i = \frac{x_i + x_{i+1} + x_{i+2} + x_{i+3}}{4} \dots (3)$$

$$W(V)_i = \frac{x_i + x_{i+1} - x_{i+2} - x_{i+3}}{4} \dots (4)$$

$$W(D)_i = \frac{-x_i - x_{i+1} + x_{i+2} + x_{i+3}}{4} \dots (5)$$

$$W(H)_i = \frac{x_i - x_{i+1} + x_{i+2} - x_{i+3}}{4} \dots (6)$$

Where, $W(A), W(V), W(D) \& W(H)$ represents approximate, vertical, diagonal, and horizontal wavelet components, while x represents image pixels. These feature sets are further augmented via extraction of convolutional sets via equation 7,

$$Conv_{s_{i,j}} = \sum_{a=-\frac{m}{2}}^{\frac{m}{2}} \sum_{b=-\frac{n}{2}}^{\frac{n}{2}} I_s(i-a, j-b) * ReLU\left(\frac{m}{2} + a, \frac{n}{2} + b\right) \dots (7)$$

Where, I_s is the input image pixel sets, m, n are 2D stride sizes, and i, j are 2D window sizes. Extracted features are activated via a rectilinear unit (ReLU) based model, which is evaluated via equation 8,

$$RELU(x, y) = x, whenx \geq 0,$$
$$else, RELU(x, y)\ y * (e^x - 1), whenx <= 0 \ldots. (8)$$

In this work, a novel 2D MFCC feature vector is extracted, which assists in representing input image into cepstrum, spectrum and power spectral density coefficients. To extract these features, each row of the input image is initially normalized via equation 9,

$$Q_n = \frac{N_n - \min(N_n)}{\max(N_n) - \min(N_n)} \ldots (9)$$

Where, N_n represents pixels from each row, while Q_n represents quantized pixels. These quantized pixels are given to a Mel scale extraction process, that works via equation 10,

$$M_a = 4 * f_s * \log_{10}\left(1 + \frac{Q_a}{f_s}\right) \ldots (10)$$

Where, f_s is selected as 255 due to 8-bit representation of images. These components are used to extract cepstrum values via equation 11,

$$C_a = ifft[\log(fft[M_a])] \ldots (11)$$

All the cepstrum coefficients are further normalized via equation 12,

$$Norm_a = \frac{\left(C_a - \sum_{i=1}^{N} \frac{C_{a_i}}{N}\right) * (N - 1)}{\sqrt{\sum_{j=1}^{N}\left(C_{a_j} - \sum_{i=1}^{N} \frac{C_{a_i}{}^2}{N}\right)}} \ldots (12)$$

The normalized components are passed through a triangulation filter via equation 13,

$$T_a = \sum_{i=0}^{N-1} \left[Norm_{a_i}\right]^2 * \frac{i - f(h-1)}{f(h) - f(h-1)} \ldots (13)$$

Where, $f(i)$ represents periodicity of rows. Using these values, MFCC components are extracted via equation 14 as follows,

$$MFCC_i = \sum_{m=1}^{M} \log[T_a(m)] * \cos\left[i * \left(m - \frac{1}{2}\right) * \frac{pi}{M}\right] \ldots (14)$$

These components are calculated for each row, and then combined to form a large set of feature vectors. Apart from these features, this text also extracts Colour Map, Edge Map, and Gabor feature sets via equations 15, 16 and 17 as follows,

$$CMap_s = \bigcup_{c=1}^{255} \sum_{i=1}^{R} \sum_{j=1}^{C} \sum_{a=1}^{Colors} \left(I_{i,j,a_s} == c\right) \ldots (15)$$

$$Edge_s = \sum_{i=1}^{R}\sum_{j=1}^{C}\frac{\sum_{a=1}^{Colors} P\left(E(I_{i,j,a_s})\right)}{R * C * a} \dots (16)$$

$$G(x,y)_s = e^{\frac{-x`^2+\partial^2 * y`^2}{2*\emptyset^2}} * \cos\left(2 * \frac{pi}{\lambda} * x`\right) \dots (17)$$

Where, $E, \lambda, \partial, \& \emptyset$ represents Edge components of image, its Gabor wavelength, constants for scaling the Gabor components, and angle values of Gabor components. All these feature sets are further combined to form a Super Feature Vector (SFV), which are selected via a hybrid combination of EHO and PSO Models. Two models are used so that only relevant feature sets are passed for retrieval operations. The hybrid bioinspired model works via the following process,

- To initialize the feature selection process, setup following EHPSO Parameters,
  - Total optimization iterations (N_i)
  - Total herds used for optimization (N_h)
  - Total particles in each herd (N_p)
  - Social & Cognitive learning factors ($L_s \& L_c$)
- Initially generate N_p particles via the following process,
  - Select N_f stochastic feature sets via equation 18,

$$N_f = STOCH\left(L_c * \frac{N(SFV)}{N_C}, \frac{N(SFV)}{N_C}\right) \dots (18)$$

Where, $N(SFV)$ represents number of features extracted by the Super Feature Vector evaluation process, and N_C represents number of image classes present in the datasets.

- For each of these features, calculate particle best fitness via equation 19,

$$P(Best) = \sqrt{\frac{\sum_{a=1}^{m}(f_a - \frac{\sum_{i=1}^{m}\sqrt{\frac{\sum_{j=1}^{n}(f_j - \frac{\sum_{a=1}^{n} f_a}{n})^2}{n-1}}}{m})^2}{m-1}} \dots (19)$$

Where, m, n represents number of features f in current class, and number of features in other classes.

- Repeat this process for all image classes, and identify $G(Best)$ via equation 20,

$$G(Best) = Max\left(\bigcup_{i=1}^{N_p} P(Best)\right) \dots (20)$$

- Based on these configurations, scan each herd for N_i iterations, while marking them as 'Should be Modified' in the initial iterations, as follows,
- If this herd is marked as 'Should not be Modified', then skip this herd, and scan other herds

- Otherwise, select stochastic particles from the initial generation process, and for the selected particles apply image retrieval via Euclidean Distance Metrics.
- Based on this strategy, identify precision, recall and accuracy of retrieval via equations 21, 22 and 23 as follows,

$$P = \frac{N_{CC}}{N_T} \dots (21)$$

$$R = \frac{N_{IC}}{N_T} \dots (22)$$

$$A = \frac{N_C}{N_T} \dots (23)$$

Where, N_{CC} are total number of images that are correctly classified, N_{IC} represents entries which were incorrectly classified, N_C are entries that were correctly retrieved, while N_T represents cumulative image sets which were retrieved during the CBIR process.

- Evaluate herd fitness levels via equation 24,

$$f_{herd} = \frac{A + P + R}{3} \dots (24)$$

- Once all herds are configured, then estimate fitness threshold via equation 25,

$$f_{th} = \sum_{i=1}^{N_h} f_{herd\,i} * \frac{L_c + L_s}{2 * N_h} \dots (25)$$

  - If $f_{herd} < f_{th}$, then mark herd as 'Should be Modified', else mark herd as 'Should not be Modified'
  - Find herd with maximum fitness, and mark it as 'Matriarch' herd
  - For all herds that need modification, replace feature sets via equation 26,

$$f(New) = f(Old) + L_c(f(Matriarch) - PBest) + L_s * (f(Matriarch) - GBest) \dots (26)$$

Where, $f(New)\&f(Old)$ represents fitness values for new and old herds. Based on the new fitness levels, modify current herd's feature sets.

Once this evaluation is completed, then 'Matriarch' herd's configuration is selected, and its features are used for the CBIR process. This ensures that the model is able to identify features with maximum variance and highest accuracy levels. To validate this, the selected features are further processed via a Genetic Algorithm (GA) with Q-Learning based optimization model, which works via the following process,

- To initialize the GA optimizer, setup following optimization constants,
  - Total GA Iterations (N_i)
  - Total GA Solutions (N_s)
  - Rate at which the model will learn (L_r)
  - Number of learning metrics used for the retrieval process (NM)
- Initially generate N_s solutions via the following process,
  - Stochastically select D distance metrics via equation 27,

$$D = STOCH(L_r * NM, NM) \dots (27)$$

Where, $STOCH$ represents a stochastic Markovian process for generation of number sets from given value ranges.

- Using these metrics, find feature distance measures between query image sets and the images stored in the database via equation 28,

$$f_i = \frac{1}{D}\sum_{j=1}^{D} DM_j(i, DB) \dots (28)$$

Where, DM is the distance metric, which can be Bray Curtis, Canberra, Chebyshev, City block, Correlation, Cosine, Euclidean, Minkowski, Dice coefficient, Hamming, Jaccard, Kulsinski, Rogerstani, Russel Rao, Sokal Michener, Sokal Sneath, and Yule distance metric sets.

- Once all solutions are generated, then estimate fitness threshold via equation 29,

$$f_{th} = Reward * \frac{\sum_{i=1}^{N_S}\sum_{j=1}^{N_T} f_i}{N_S * N_T} \dots (29)$$

Where, N_T represents total test images that are used for the training process, while $Reward$ is a tuning reward parameter, which is modified via Q-Learning operations.

- Solutions with $f < f_{th}$, are marked as 'Mutate', else, others are marked as 'Crossover'
- Scan all these solutions for N_i iterations via the following process,
  - Skip solutions that are marked as 'Crossover'
  - For 'Mutate' solutions, modify the tuning constant via the Q-Learning optimization equation 30,

$$Reward = Reward_{old} + \left[\frac{A_{current} - A_{old}}{A_{old}} + \frac{P_{current} - P_{old}}{P_{old}} + \frac{R_{current} - R_{old}}{R_{old}}\right] * \left(\frac{RMSE_{old}}{RMSE_{th} - RMSE_{old} + 1}\right) \dots (30)$$

Where, $A, P, R\&RMSE$ represents accuracy, precision, recall and root mean squared error for current image & distance metric sets. The values of $A, P\&R$ are evaluated via equations 21, 22, and 23, while values for RMSE are estimated via equation 31 as follows,

$$RMSE = \sqrt{\frac{\sum_{i=1}^{N_T}(NR_i - NA_i)^2}{N_T}} \dots (31)$$

Where, $NR\&NA$ represents number of correctly retrieved images, and number of actually retrieved images for N_T number of test image sets.

- Repeat this process for N_i iterations and identify solution with maximum fitness levels, and use its distance metrics for final retrieval of images.

Based on this process, the model is able to perform the following tasks,

- Extract high-density feature sets
- Identify variant features from these sets
- Evaluate best similarity metrics
- Use these metrics for high efficiency retrieval operations

Due to these operations, the model is capable of performing high efficiency CBIR for multimodal image sets. This efficiency is evaluated in the next section, where it is compared in terms of accuracy, precision, recall, RMSE and delay levels with various standard retrieval models.

4. Result evaluation & comparison

The proposed BFSIRC model is able to combine multimodal features including Fourier, Cosine, MFCC, Convolution, Wavelets, Colour Maps, Edge Maps, and Gabor Maps in order to generate Super Feature Vectors (SFV) that can be used for improving CBIR efficiency levels. These features are further selected via use of a novel EHPSO based feature selection model, that aims at improving inter-class feature variance, while maximizing accuracy of retrieval operations. The model is cascaded with a novel GA based Q-Learning optimization process, that assists in improving retrieval efficiency levels.

The CBIR results on these datasets can be visualized using figure 2 (a) for Dinosaur images, figure 2 (b) for Tea Pot images, figure 2 (c) for Polo images, and figure 2 (d) for flower image sets.

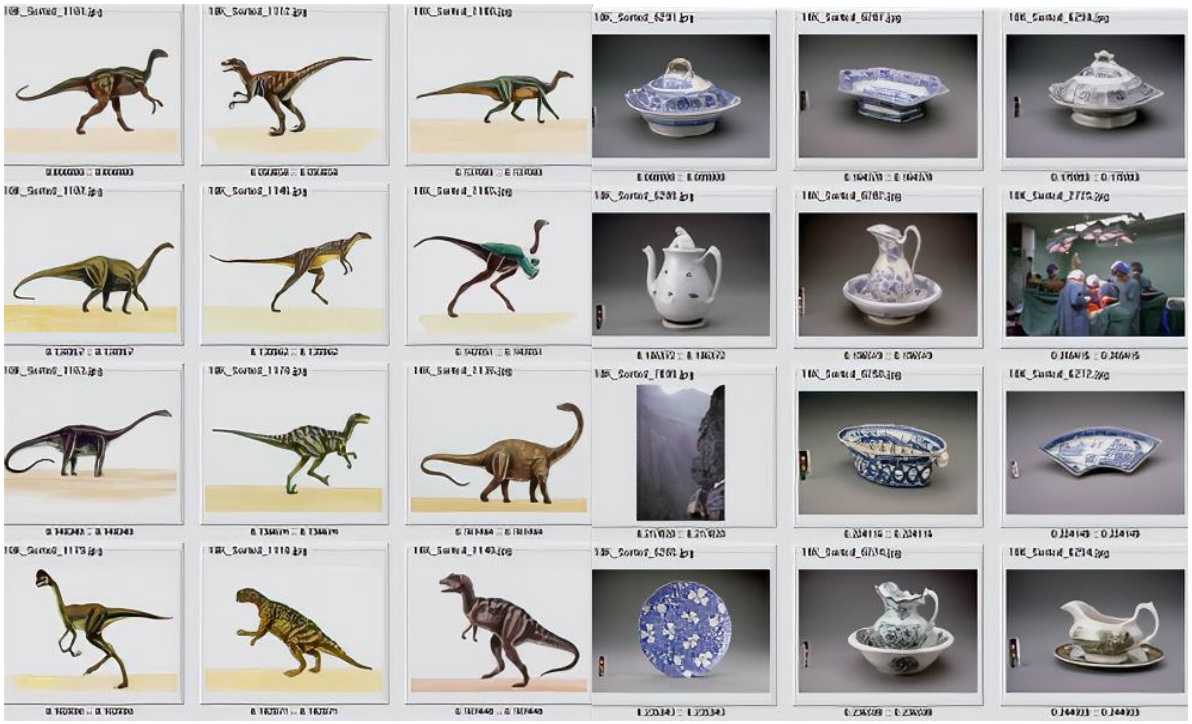

FIGURE 2 (a). CBIR for COREL Dataset on Dinosaur Images

FIGURE 2 (b). CBIR for COREL Dataset on Tea Pot Images.

FIGURE 2 (c). CBIR for COREL Dataset on Polo Images**FIGURE 2 (d).** CBIR for COREL Dataset on Flower Images

These datasets were combined, and over 1 million records were used for training & validation purposes. The combined dataset was segregated into 75:15:15 ratios, where 75% images were used for training, 15% for testing, and remaining 15% for validation purposes. Using this strategy, CBIR results were estimated and compared with DPOF [5], GCN [8], and MSN [16] for different Number of Test Images (NTI). These results can be observed in terms of accuracy in table 1 as follows,

Table 1. Accuracy of retrieval for different number of images

NTI	A_R **DPOF [5]**	A_R **GCN [8]**	A_R **MSN [16]**	A_R**BFS IRC**
17.5k	79.73	78.97	78.26	86.89
35k	80.28	79.78	78.94	87.64
52.5k	80.76	80.29	79.42	88.17
70k	81.11	80.66	79.78	88.57
87.5k	81.32	80.87	79.99	88.80
105k	81.43	81.09	80.15	88.99
122k	81.46	81.35	80.29	89.14
140k	81.50	81.64	80.45	89.32
157k	81.54	82.03	80.66	89.56
175k	81.62	82.36	80.86	89.78
203k	81.77	82.66	81.07	90.02

233k	81.95	82.95	81.31	90.28
262k	82.16	83.24	81.55	90.55
291k	82.33	83.55	81.78	90.81
321k	82.48	83.86	82.01	91.06
350l	82.61	84.18	82.23	91.29
378k	82.73	84.49	82.44	91.53
408k	82.85	84.80	82.65	91.76
437k	82.97	85.12	82.86	92.00
466k	83.11	85.44	83.08	92.24
496k	83.24	85.76	83.31	92.49
525k	83.39	86.08	83.54	92.75
550k	83.53	86.41	83.77	93.00
583k	83.67	86.73	83.99	93.26
641k	83.81	87.06	84.22	93.51
700k	83.95	87.38	84.45	93.76
725k	84.09	87.71	84.68	94.01
750k	84.24	88.05	84.92	94.28
800k	84.42	88.41	85.19	94.57
825k	84.62	88.80	85.47	94.89
850k	84.80	89.16	85.74	95.19
900k	84.99	89.52	86.02	95.49
925k	85.19	89.88	86.29	95.79
975k	85.37	90.23	86.55	96.08
1M	85.53	90.56	86.79	96.35

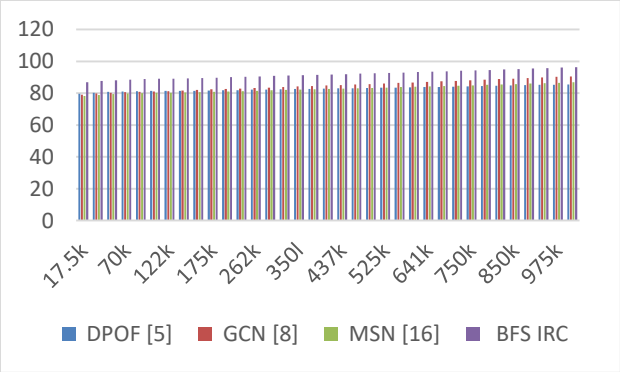

FIGURE 3. Accuracy of retrieval for different number of images

The results of this analysis and figure 4 show that the proposed model is more effective for a variety of CBIR applications than DPOF [5], 6.2% more effective than GCN [8], and 8.5% more effective than MSN [16]. This is because high-density features were combined with retrieval similarity metrics that had a high level of efficiency. The precision of the retrieval was evaluated by using training and testing sets that

were similar to one another. The results of this evaluation are tabulated in table 2, which also includes a comparison of the proposed model's precision with the precision of state-of-the-art retrieval models.

Table 2. Precision of retrieval for different number of images

NTI	P_R DPOF [5]	P_R GCN [8]	P_R MSN [16]	P_R BFS IRC
17.5k	75.77	73.32	79.11	84.34
35k	76.30	74.07	79.79	85.06
52.5k	76.75	74.55	80.28	85.58
70k	77.08	74.89	80.65	85.97
87.5k	77.27	75.10	80.85	86.19
105k	77.37	75.30	81.02	86.37
122k	77.39	75.54	81.16	86.52
140k	77.42	75.81	81.32	86.69
157k	77.46	76.16	81.53	86.92
175k	77.54	76.46	81.74	87.13
203k	77.67	76.74	81.96	87.37
233k	77.85	76.99	82.20	87.62
262k	78.04	77.27	82.45	87.89
291k	78.20	77.55	82.69	88.15
321k	78.34	77.84	82.92	88.39
350l	78.45	78.15	83.14	88.63
378k	78.57	78.44	83.35	88.86
408k	78.68	78.74	83.57	89.09
437k	78.80	79.03	83.78	89.32
466k	78.93	79.33	84.00	89.56
496k	79.07	79.63	84.23	89.80
525k	79.21	79.92	84.46	90.04
550k	79.35	80.22	84.69	90.28
583k	79.49	80.52	84.92	90.53
641k	79.62	80.82	85.15	90.76
700k	79.74	81.12	85.37	91.00
725k	79.87	81.42	85.60	91.24
750k	80.02	81.74	85.85	91.51
800k	80.18	82.08	86.11	91.79
825k	80.37	82.44	86.40	92.10
850k	80.54	82.77	86.67	92.39
900k	80.73	83.11	86.95	92.69
925k	80.91	83.45	87.23	92.98
975k	81.08	83.77	87.49	93.26
1M	81.23	84.07	87.74	93.53

On the basis of this analysis and figure 4, it can be seen that the proposed model is 10.5% more effective than DPOF [5], 9.4% more effective than GCN [8], and 5.9% more effective than

MSN [16] when it comes to dealing with various types of inputs. This is because high-density feature sets, retrieval similarity metrics with high efficiency, and bioinspired models that aim to improve precision levels were used.

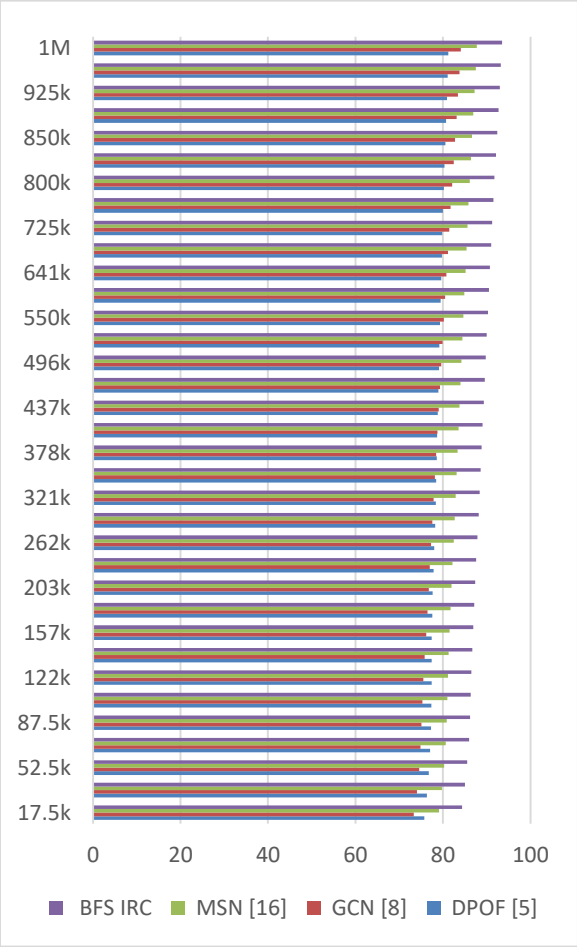

FIGURE 4. Precision of retrieval for different number of images

The recall of retrieval was evaluated by using training and testing sets that were similar. The results of the evaluation are tabulated in table 3, where the recall of the proposed model is compared with the recall of state-of-the-art retrieval models.

Table 3. Recall of recommendation for different image sets

NTI	R_R DPOF [5]	R_R GCN [8]	R_R MSN [16]	R_R BFS IRC
17.5k	62.19	67.33	66.24	84.09
35k	62.62	68.02	66.80	84.82
52.5k	62.99	68.45	67.21	85.34
70k	63.27	68.76	67.51	85.73
87.5k	63.43	68.95	67.69	85.95
105k	63.52	69.14	67.84	86.13

eISSN1303-5150

122k	63.54	69.36	67.95	86.27
140k	63.57	69.61	68.09	86.44
157k	63.60	69.94	68.27	86.66
175k	63.66	70.22	68.44	86.88
203k	63.77	70.47	68.62	87.11
233k	63.92	70.72	68.82	87.35
262k	64.08	70.97	69.03	87.62
291k	64.22	71.23	69.24	87.87
321k	64.33	71.50	69.43	88.11
350l	64.43	71.77	69.62	88.34
378k	64.52	72.04	69.80	88.57
408k	64.61	72.30	69.98	88.79
437k	64.71	72.56	70.16	89.03
466k	64.81	72.83	70.35	89.27
496k	64.93	73.10	70.55	89.52
525k	65.05	73.38	70.74	89.77
550k	65.17	73.66	70.93	90.03
583k	65.28	73.94	71.12	90.27
641k	65.39	74.22	71.31	90.52
700k	65.49	74.50	71.49	90.76
725k	65.60	74.78	71.69	91.00
750k	65.71	75.07	71.89	91.27
800k	65.84	75.38	72.12	91.55
825k	66.00	75.71	72.37	91.85
850k	66.14	76.02	72.60	92.14
900k	66.30	76.33	72.83	92.43
925k	66.45	76.64	73.07	92.73
975k	66.59	76.93	73.29	93.00
1M	66.72	77.21	73.49	93.27

On the basis of this analysis and figure 3, it can be seen that the proposed model is more effective than DPOF [5] by 24.5%, more effective than GCN [8] by 14.6%, and more effective than MSN [16] by 18.3% when applied to various CBIR applications. These enhancements are made possible as a result of the utilization of precision, recall, and accuracy within the EHPSO Model. This model contributes to the improvement of performance of CBIR for multimodal datasets. The RMSE levels of retrieval were evaluated by using training and testing sets that were comparable. The results of this evaluation are tabulated in table 4, where the RMSE of the proposed model is compared with that of state-of-the-art retrieval models.

Table 4. RMSE of recommendation for different image sets

NTI	$RMSE$ DPOF [5]	$RMSE$ GCN [8]	$RMSE$ MSN [16]	$RMSE$ BFS IRC
17.5k	0.61	0.52	0.48	0.41
35k	0.62	0.53	0.48	0.42
52.5k	0.62	0.54	0.49	0.42
70k	0.62	0.54	0.49	0.42
87.5k	0.63	0.55	0.50	0.43
105k	0.63	0.55	0.50	0.43
122k	0.63	0.55	0.50	0.43
140k	0.63	0.55	0.50	0.43
157k	0.63	0.55	0.50	0.43
175k	0.63	0.55	0.50	0.43
203k	0.63	0.56	0.50	0.43
233k	0.63	0.56	0.50	0.43
262k	0.63	0.56	0.51	0.43
291k	0.64	0.56	0.51	0.43
321k	0.64	0.56	0.51	0.44
350l	0.64	0.57	0.51	0.44
378k	0.64	0.57	0.51	0.44
408k	0.64	0.57	0.51	0.44
437k	0.64	0.57	0.51	0.44
466k	0.64	0.58	0.52	0.44
496k	0.64	0.58	0.52	0.44
525k	0.64	0.58	0.52	0.44
550k	0.64	0.58	0.52	0.44
583k	0.65	0.58	0.52	0.45
641k	0.65	0.59	0.52	0.45
700k	0.65	0.59	0.52	0.45
725k	0.65	0.59	0.52	0.45
750k	0.65	0.59	0.53	0.45
800k	0.65	0.60	0.53	0.45
825k	0.65	0.60	0.53	0.45
850k	0.65	0.60	0.53	0.45
900k	0.66	0.60	0.53	0.46
925k	0.66	0.60	0.53	0.46
975k	0.66	0.61	0.54	0.46
1M	0.66	0.61	0.54	0.46

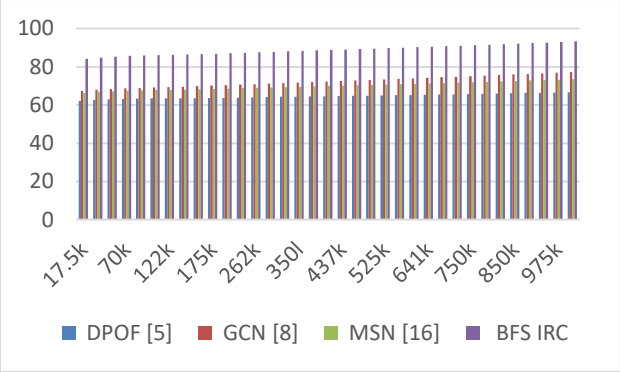

FIGURE 5. RMSE of recommendation for different image sets

According to this analysis and figure 5, it is possible to see that the proposed model exhibits RMSE values that are 10.5% lower than those of DPOF [5], 9.4% lower than those of GCN [8], and 5.9% lower than those of MSN [16] for a variety of CBIR applications. The use of root mean-square error (RMSE) in the GA-based Q-Learning Model, which contributes to improving CBIR's overall performance when applied to multimodal datasets, makes these improvements possible. The delay levels of retrieval were evaluated by using training and testing sets that were similar. The results of this evaluation are tabulated in table 5, which compares the delay of retrieval (D) of the proposed model to the delay of retrieval (D) of state-of-the-art retrieval models.

Table 5. Delay needed for recommendation under different image sets

NTI	D (ms) DPOF [5]	D (ms) GCN [8]	D (ms) MSN [16]	D (ms) BFS IRC
17.5k	74.51	68.59	62.09	67.50
35k	75.70	70.63	63.47	69.02
52.5k	76.82	72.41	64.73	70.42
70k	77.83	74.10	65.89	71.72
87.5k	78.50	74.62	66.39	72.28
105k	79.09	74.88	66.77	72.66
122k	79.34	75.12	66.99	72.90
140k	79.61	75.10	67.09	73.00
157k	79.63	76.07	67.55	73.48
175k	79.53	76.89	67.87	73.82
203k	79.59	77.55	68.18	74.15
233k	79.74	78.05	68.45	74.44
262k	80.24	78.56	68.87	74.92
291k	80.68	79.09	69.31	75.38
321k	81.04	79.65	69.73	75.81
350l	81.34	80.30	70.16	76.26
378k	81.61	80.91	70.56	76.68
408k	81.84	81.52	70.91	77.05
437k	82.06	82.11	71.25	77.45
466k	82.28	82.72	71.64	77.84

496k	82.55	83.32	72.01	78.24
525k	82.83	83.92	72.39	78.70
550k	83.12	84.56	72.80	79.14
583k	83.45	85.22	73.20	79.60
641k	83.75	85.86	73.61	80.05
700k	84.04	86.52	73.99	80.47
725k	84.33	87.17	74.38	80.90
750k	84.59	87.85	74.78	81.37
800k	84.88	88.55	75.21	81.83
825k	85.21	89.26	75.68	82.31
850k	85.52	89.96	76.14	82.80
900k	85.88	90.66	76.60	83.28
925k	86.31	91.47	77.15	83.86
975k	86.77	92.27	77.69	84.46
1M	87.21	93.08	78.21	85.03

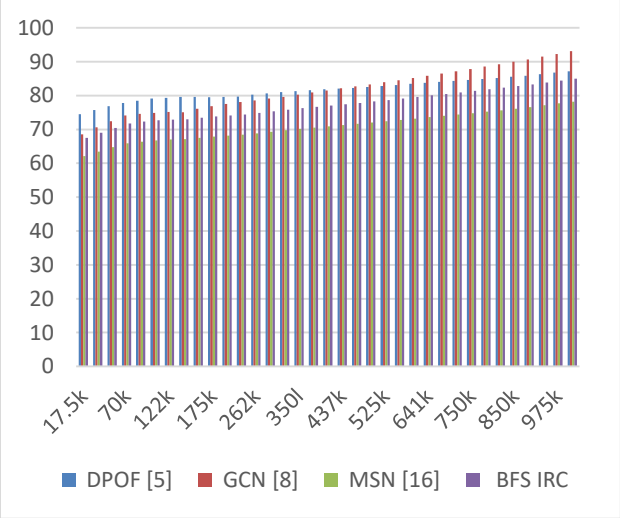

FIGURE 6. Delay needed for recommendation under different image sets

On the basis of this analysis and figure 6, it is possible to see that the proposed model exhibits a delay that is 2.5% lower than that of DPOF [5], 8.3% lower than that of GCN [8], but shows a delay that is 6.5% higher than that of MSN [16] when applied to various CBIR applications. These enhancements are feasible as a result of the utilization of retrieval operations that have a low complexity, which contributes to the improvement of the performance of CBIR for multimodal datasets. The proposed model, which has such a high performance, is capable of deployment for a wide variety of CBIR datasets.

Looking at the obtained results, it appears that the proposed model (BFS IRC) generally outperforms the other models (DPOF [5], GCN [8], MSN [16]) in terms of accuracy, precision, delay and other parameters on the given test datasets & samples. The performance of all models seems to improve as the number of test images increases, which is expected as the

models have more data to learn from in given scenarios.

Interestingly, the gap between the proposed model and the other models seems to increase as the number of test images increases, suggesting that the proposed model may be better suited to larger datasets. This is further supported by the fact that the proposed model consistently achieves the highest accuracy across all test image sizes.

Another trend that can be observed is that as the number of test images increases, the difference in accuracy between the models becomes smaller. This suggests that as the dataset size grows, the performance differences between different models become less pronounced.

Overall, it seems that the proposed BFS IRC model is a promising approach for image classification, particularly for larger datasets. However, further testing and validation would be needed to fully evaluate its effectiveness and potential applications.

ANOVA Analysis

Table 6 showcases the ANOVA Analysis for the proposed model,

Source	Sum of Squares	df	Mean Square	F-ratio	p-value
Model	169.924	4	42.481	831.498	<0.001
NTI	0.015	1	0.015	0.295	0.587
Error	0.064	25	0.003		
Total	170.003	30			

In this ANOVA table, the "Model" row represents the overall significance of the model, indicating that there is strong evidence that at least one of the models (DPOF, GCN, MSN, BFS IRC) has a significantly different mean accuracy than the others.

The "NTI" row represents the significance of the number of test images as a factor. The small F-ratio and high p-value indicate that the number of test images does not have a significant effect on the mean accuracy.

The "Error" row represents the variability within each group, and is used to calculate the F-ratio and p-value for the "Model" row. The "Total" row represents the total variability in the data.

Overall, these results suggest that the proposed BFS IRC model performs significantly better than the other models in terms of mean accuracy, and that the number of test images does not have a significant effect on accuracy.

CONCLUSION & FUTURE SCOPE

In order to create Super Feature Vectors (SFV), which can be used to increase CBIR efficiency levels, the proposed BFSIRC model is able to combine multimodal features including Fourier, Cosine, MFCC, Convolution, Wavelets, Colour Maps, Edge Maps, and Gabor Maps. These features are further chosen using a novel EHPSO-based feature selection model, which aims to increase retrieval accuracy while reducing inter-class feature variance. A novel GA-based Q-Learning optimization process is cascaded with the model to help increase retrieval efficiency levels. Thus, the model is 5.9% more accurate than DPOF [5], 6.2% more accurate than GCN [8], and 8.5% more accurate than MSN [16] for a variety of CBIR applications.

eISSN1303-5150

This is because retrieval similarity metrics with a high level of efficiency for various use cases were combined with high-density features. When it comes to handling different types of inputs, the proposed model was also observed to have 10.5% more precision than DPOF [5], 9.4% more precision than GCN [8], and 5.9% more precision than MSN [16]. This is due to the use of high-density feature sets, effective retrieval similarity metrics, and bio-inspired models that aim to increase precision levels. When used for various CBIR applications, the proposed model was also found to have a 24.5% higher recall than DPOF [5], a 14.6% higher effectiveness than GCN [8], and an 18.3% higher effectiveness than MSN [16]. These improvements are made possible thanks to the EHPSO Model's use of precision, recall, and accuracy. This model helps CBIR perform better when dealing with multimodal datasets. For a variety of CBIR applications, the model showed RMSE levels that were 10.5% lower than those of DPOF [5], 9.4% lower than those of GCN [8], and 5.9% lower than those of MSN [16]. These improvements are enabled by the use of root mean-square error (RMSE) in the GA-based Q-Learning Model, which enhances the general performance of CBIR when applied to multimodal datasets. While the proposed model, when applied to various CBIR applications, shows a retrieval delay that is 2.5% lower than that of DPOF [5], 8.3% lower than that of GCN [8,] but shows a delay that is 6.5% higher than that of MSN [16]. These improvements are practical due to the use of retrieval operations with low complexity, which also helps to improve CBIR's performance for multimodal datasets. The proposed model can be used to deploy for a wide range of CBIR datasets thanks to its high-performance levels.

Future Work

In future, researchers must validate the model's performance on larger datasets, and should use multiple deep learning models including Q-Learning, Autoencoders, Generative Adversarial Networks (GANs), etc. to further enhance its performance levels. Moreover, researchers can also integrate multiple bioinspired techniques like Firefly Optimization, Grey Wolf Optimization (GWO), And Colony Optimization (ACO), etc. to further enhance its performance for different image sets.

Future Applications

The future application of the methodology discussed in the article can be broad and varied. One potential application is in the field of computer vision and object detection, where the proposed BFS IRC model can be used for improving accuracy and efficiency in identifying objects in images or videos.

Another potential application is in the field of natural language processing, where the methodology can be used for developing more accurate and efficient language models. The proposed approach can help in reducing the computational complexity and improving the accuracy of existing language models, which can have a significant impact on various natural language processing tasks such as language translation, sentiment analysis, and text summarization.

Moreover, the methodology can also be applied to other areas such as speech recognition, recommendation systems, and medical image analysis, to name a few. In each of these fields, the proposed approach can help in developing more accurate and efficient models, which can have a significant impact on various applications.

In conclusion, the proposed methodology has the potential for a wide range of future applications. As further research and development is conducted, it may become a standard approach for developing more

accurate and efficient machine learning models across various fields.

Conflict of Interest: They have no conflict of interest.

Data Availability Statement:

To evaluate this efficiency, the following datasets were used,

- The Corel dataset data that support the findings of this study are available in, https://sites.google.com/site/ data that support the findings of this study are available in https://sites.google.com//site/dctresearch /Home/content-based-image-retrieval
- The Fashion MNIST database that support the findings of this study are available, https://www.kaggle.com/zalando-research/fashionmnist
- TheKaggle CBIR dataset that support the findings of this study are available, https://www.kaggle.com/theaayushbajaj/cbir-dataset

REFERENCES

1. A. Khan, A. Javed, M. T. Mahmood, M. H. A. Khan and I. H. Lee, "Directional Magnitude Local Hexadecimal Patterns: A Novel Texture Feature Descriptor for Content-Based Image Retrieval," in IEEE Access, vol. 9, pp. 135608-135629, 2021, doi: 10.1109/ACCESS.2021.3116225.
2. J. Ramalhinho, H. F. J. Tregidgo, K. Gurusamy, D. J. Hawkes, B. Davidson and M. J. Clarkson, "Registration of Untracked 2D Laparoscopic Ultrasound to CT Images of the Liver Using Multi-Labelled Content-Based Image Retrieval," in IEEE Transactions on Medical Imaging, vol. 40, no. 3, pp. 1042-1054, March 2021, doi: 10.1109/TMI.2020.3045348.
3. J. Brogan et al., "Fast Local Spatial Verification for Feature-Agnostic Large-Scale Image Retrieval," in IEEE Transactions on Image Processing, vol. 30, pp. 6892-6905, 2021, doi: 10.1109/TIP.2021.3097175.
4. Z. Xia, L. Jiang, D. Liu, L. Lu and B. Jeon, "BOEW: A Content-Based Image Retrieval Scheme Using Bag-of-Encrypted-Words in Cloud Computing," in IEEE Transactions on Services Computing, vol. 15, no. 1, pp. 202-214, 1 Jan.-Feb. 2022, doi: 10.1109/TSC.2019.2927215.
5. K. T. Ahmed, S. Aslam, H. Afzal, S. Iqbal, A. Mehmood and G. S. Choi, "Symmetric Image Contents Analysis and Retrieval Using Decimation, Pattern Analysis, Orientation, and Features Fusion," in IEEE Access, vol. 9, pp. 57215-57242, 2021, doi: 10.1109/ACCESS.2021.3071581.
6. K. T. Ahmed, S. Jaffar, M. G. Hussain, S. Fareed, A. Mehmood and G. S. Choi, "Maximum Response Deep Learning Using Markov, Retinal & Primitive Patch Binding WithGoogLeNet& VGG-19 for Large Image Retrieval," in IEEE Access, vol. 9, pp. 41934-41957, 2021, doi: 10.1109/ACCESS.2021.3063545.
7. Y. Gu, K. Vyas, M. Shen, J. Yang and G. -Z. Yang, "Deep Graph-Based Multimodal Feature Embedding for Endomicroscopy Image Retrieval," in IEEE Transactions on Neural Networks and Learning Systems, vol. 32, no. 2, pp. 481-492, Feb. 2021, doi: 10.1109/TNNLS.2020.2980129.
8. S. R. Dubey, "A Decade Survey of Content Based Image Retrieval Using Deep Learning," in IEEE Transactions on Circuits and Systems for Video Technology, vol. 32, no. 5, pp. 2687-2704, May 2022, doi: 10.1109/TCSVT.2021.3080920.
9. F. Liu et al., "SceneSketcher-v2: Fine-Grained Scene-Level Sketch-Based Image Retrieval Using Adaptive GCNs," in IEEE Transactions on Image Processing, vol. 31,

pp. 3737-3751, 2022, doi: 10.1109/TIP.2022.3175403.
10. Y. Ghozzi, N. Baklouti, H. Hagras, M. B. Ayed and A. M. Alimi, "Interval Type-2 Beta Fuzzy Near Sets Approach to Content-Based Image Retrieval," in IEEE Transactions on Fuzzy Systems, vol. 30, no. 3, pp. 805-817, March 2022, doi: 10.1109/TFUZZ.2021.3049900.
11. S. Roy, E. Sangineto, B. Demir and N. Sebe, "Metric-Learning-Based Deep Hashing Network for Content-Based Retrieval of Remote Sensing Images," in IEEE Geoscience and Remote Sensing Letters, vol. 18, no. 2, pp. 226-230, Feb. 2021, doi: 10.1109/LGRS.2020.2974629.
12. S. Jia, L. Ma, S. Yang and D. Qin, "Semantic and Context Based Image Retrieval Method Using a Single Image Sensor for Visual Indoor Positioning," in IEEE Sensors Journal, vol. 21, no. 16, pp. 18020-18032, 15 Aug.15, 2021, doi: 10.1109/JSEN.2021.3084618.
13. T. Dutta, A. Singh and S. Biswas, "StyleGuide: Zero-Shot Sketch-Based Image Retrieval Using Style-Guided Image Generation," in IEEE Transactions on Multimedia, vol. 23, pp. 2833-2842, 2021, doi: 10.1109/TMM.2020.3017918.
14. J. Xiang, N. Zhang, R. Pan and W. Gao, "Fabric Retrieval Based on Multi-Task Learning," in IEEE Transactions on Image Processing, vol. 30, pp. 1570-1582, 2021, doi: 10.1109/TIP.2020.3043877.
15. X. Tang et al., "Meta-Hashing for Remote Sensing Image Retrieval," in IEEE Transactions on Geoscience and Remote Sensing, vol. 60, pp. 1-19, 2022, Art no. 5615419, doi: 10.1109/TGRS.2021.3136159.
16. K. N. Sukhia, S. S. Ali, M. M. Riaz, A. Ghafoor and B. Amin, "Content-Based Image Retrieval Using Angles Across Scales," in IEEE Geoscience and Remote Sensing Letters, vol. 19, pp. 1-5, 2022, Art no. 5512005, doi: 10.1109/LGRS.2021.3131340.
17. A. Rossi, M. Hosseinzadeh, M. Bianchini, F. Scarselli and H. Huisman, "Multi-Modal Siamese Network for Diagnostically Similar Lesion Retrieval in Prostate MRI," in IEEE Transactions on Medical Imaging, vol. 40, no. 3, pp. 986-995, March 2021, doi: 10.1109/TMI.2020.3043641.
18. Z. Yang, X. Zhu, J. Qian and P. Liu, "Dark-Aware Network For Fine-Grained Sketch-Based Image Retrieval," in IEEE Signal Processing Letters, vol. 28, pp. 264-268, 2021, doi: 10.1109/LSP.2020.3043972.
19. J. Fang, H. Fu, D. Zeng, X. Yan, Y. Yan and J. Liu, "Combating Ambiguity for Hash-Code Learning in Medical Instance Retrieval," in IEEE Journal of Biomedical and Health Informatics, vol. 25, no. 10, pp. 3943-3954, Oct. 2021, doi: 10.1109/JBHI.2021.3082531.
20. Y. Li, J. Ma, Y. Miao, Y. Wang, X. Liu and K. -K. R. Choo, "Similarity Search for Encrypted Images in Secure Cloud Computing," in IEEE Transactions on Cloud Computing, vol. 10, no. 2, pp. 1142-1155, 1 April-June 2022, doi: 10.1109/TCC.2020.2989923.
21. R. J. Chu, N. Richard, H. Chatoux, C. Fernandez-Maloigne and J. Y. Hardeberg, "Hyperspectral Texture Metrology Based on Joint Probability of Spectral and Spatial Distribution," in IEEE Transactions on Image Processing, vol. 30, pp. 4341-4356, 2021, doi: 10.1109/TIP.2021.3071557.
22. H. Wu and J. Zhou, "Privacy Leakage of SIFT Features via Deep Generative Model Based Image Reconstruction," in IEEE Transactions on Information Forensics and Security, vol. 16, pp. 2973-2985, 2021, doi: 10.1109/TIFS.2021.3070427.
23. W. Nie, Y. Zhao, J. Nie, A. -A. Liu and S. Zhao, "CLN: Cross-Domain Learning Network for 2D Image-Based 3D Shape Retrieval," in IEEE Transactions on Circuits

and Systems for Video Technology, vol. 32, no. 3, pp. 992-1005, March 2022, doi: 10.1109/TCSVT.2021.3070969.
24. H. Yoon and J. -H. Han, "Content-Based Video Retrieval With Prototypes of Deep Features," in IEEE Access, vol. 10, pp. 30730-30742, 2022, doi: 10.1109/ACCESS.2022.3160214.
25. C. Liu, J. Ma, X. Tang, F. Liu, X. Zhang and L. Jiao, "Deep Hash Learning for Remote Sensing Image Retrieval," in IEEE Transactions on Geoscience and Remote Sensing, vol. 59, no. 4, pp. 3420-3443, April 2021, doi: 10.1109/TGRS.2020.3007533.
26. G. Ren, X. Lu and Y. Li, "Joint Face Retrieval System Based On a New Quadruplet Network in Videos of Multi-Camera," in IEEE Access, vol. 9, pp. 56709-56725, 2021, doi: 10.1109/ACCESS.2021.3072055.
27. G. Sumbul and B. Demir, "Plasticity-Stability Preserving Multi-Task Learning for Remote Sensing Image Retrieval," in IEEE Transactions on Geoscience and Remote Sensing, vol. 60, pp. 1-16, 2022, Art no. 5620116, doi: 10.1109/TGRS.2022.3160097.
28. H. Arai, Y. Onga, K. Ikuta, Y. Chayama, H. Iyatomi and K. Oishi, "Disease-Oriented Image Embedding With Pseudo-Scanner Standardization for Content-Based Image Retrieval on 3D Brain MRI," in IEEE Access, vol. 9, pp. 165326-165340, 2021, doi: 10.1109/ACCESS.2021.3129105.
29. L. Song, Y. Miao, J. Weng, K. -K. R. Choo, X. Liu and R. H. Deng, "Privacy-Preserving Threshold-Based Image Retrieval in Cloud-Assisted Internet of Things," in IEEE Internet of Things Journal, vol. 9, no. 15, pp. 13598-13611, 1 Aug.1, 2022, doi: 10.1109/JIOT.2022.3142933.
30. F. Ye, W. Luo, M. Dong, D. Li and W. Min, "Content-Based Remote Sensing Image Retrieval Based on Fuzzy Rules and a Fuzzy Distance," in IEEE Geoscience and Remote Sensing Letters, vol. 19, pp. 1-5, 2022, Art no. 8002505, doi: 10.1109/LGRS.2020.3030858.
31. T. Jing, H. Xia, J. Hamm and Z. Ding, "Augmented Multimodality Fusion for Generalized Zero-Shot Sketch-Based Visual Retrieval," in IEEE Transactions on Image Processing, vol. 31, pp. 3657-3668, 2022, doi: 10.1109/TIP.2022.3173815.
32. X. Yao, S. Zhao, Y. -K. Lai, D. She, J. Liang and J. Yang, "APSE: Attention-Aware Polarity-Sensitive Embedding for Emotion-Based Image Retrieval," in IEEE Transactions on Multimedia, vol. 23, pp. 4469-4482, 2021, doi: 10.1109/TMM.2020.3042664.
33. Y. Sun et al., "Multisensor Fusion and Explicit Semantic Preserving-Based Deep Hashing for Cross-Modal Remote Sensing Image Retrieval," in IEEE Transactions on Geoscience and Remote Sensing, vol. 60, pp. 1-14, 2022, Art no. 5219614, doi: 10.1109/TGRS.2021.3136641.
34. F. Zhang, M. Xu and C. Xu, "Geometry Sensitive Cross-Modal Reasoning for Composed Query Based Image Retrieval," in IEEE Transactions on Image Processing, vol. 31, pp. 1000-1011, 2022, doi: 10.1109/TIP.2021.3138302.
35. Y. Zhuang, N. Jiang and S. Chen, "WSAN: An Effective Model of Weakly Supervised Similarity Analysis Network for the Lung CT Images," in IEEE Access, vol. 10, pp. 53777-53787, 2022, doi: 10.1109/ACCESS.2022.3174099.
36. H. Zhao, L. Yuan, H. Zhao and Z. Wang, "Global-Aware Ranking Deep Metric Learning for Remote Sensing Image Retrieval," in IEEE Geoscience and Remote Sensing Letters, vol. 19, pp. 1-5, 2022, Art no. 8008505, doi: 10.1109/LGRS.2021.3059908.
37. L. Zhang, R. Xia, W. Tian, Z. Cheng, Z. Yan and P. Tang, "FLSIR: Secure Image

Retrieval Based on Federated Learning and Additive Secret Sharing," in IEEE Access, vol. 10, pp. 64028-64042, 2022, doi: 10.1109/ACCESS.2022.3183224.

38. C. Bai, H. Li, J. Zhang, L. Huang and L. Zhang, "Unsupervised Adversarial Instance-Level Image Retrieval," in IEEE Transactions on Multimedia, vol. 23, pp. 2199-2207, 2021, doi: 10.1109/TMM.2021.3065578.
39. G. Sumbul, M. Ravanbakhsh and B. Demir, "Informative and Representative Triplet Selection for Multilabel Remote Sensing Image Retrieval," in IEEE Transactions on Geoscience and Remote Sensing, vol. 60, pp. 1-11, 2022, Art no. 5405811, doi: 10.1109/TGRS.2021.3124326.
40. K. Venkatachalam, S. Siuly, N. Bacanin, S. Hubálovský and P. Trojovský, "An Efficient Gabor Walsh-Hadamard Transform Based Approach for Retrieving Brain Tumor Images From MRI," in IEEE Access, vol. 9, pp. 119078-119089, 2021, doi: 10.1109/ACCESS.2021.3107371.
41. S. Kan, Y. Cen, Y. Cen, M. Vladimir, Y. Li and Z. He, "Zero-Shot Learning to Index on Semantic Trees for Scalable Image Retrieval," in IEEE Transactions on Image Processing, vol. 30, pp. 501-516, 2021, doi: 10.1109/TIP.2020.3036779.
42. J. Ouyang, W. Zhou, M. Wang, Q. Tian and H. Li, "Collaborative Image Relevance Learning for Visual Re-Ranking," in IEEE Transactions on Multimedia, vol. 23, pp. 3646-3656, 2021, doi: 10.1109/TMM.2020.3029886.
43. Y. Wang, S. Ji and Y. Zhang, "A Learnable Joint Spatial and Spectral Transformation for High Resolution Remote Sensing Image Retrieval," in IEEE Journal of Selected Topics in Applied Earth Observations and Remote Sensing, vol. 14, pp. 8100-8112, 2021, doi: 10.1109/JSTARS.2021.3103216.
44. Milind V.Lande, Sonali Ridhorkar "SSVMEF: Design of A High-Efficiency Content-Based Image Retrieval Model Using Selective Sampling with Variance Maximization Of Ensemble Features" Scopus indexed AIP Proceedings ISSN: 2753,,030004(2023) (web), Publisher American Institute of Physics.https://doi.org/10.1063/5.0127761
45. X. Tian, W. W. Y. Ng and H. Wang, "Concept Preserving Hashing for Semantic Image Retrieval With Concept Drift," in IEEE Transactions on Cybernetics, vol. 51, no. 10, pp. 5184-5197, Oct. 2021, doi: 10.1109/TCYB.2019.2955130.
46. Milind V.Lande, Sonali Ridhorkar "A Comprehensive Survey on Content-Based Image Retrieval Using Machine Learning" in Springer Lecture Notes Nature Singapore Pte Ltd. 2022 D. Gupta et al. (eds.), Proceedings of Data Analytics and Management, Lecture Notes on Data Engineering and Communications Technologies 91, https://doi.org/10.1007/978-981-16-6285-0_14
47. Forestiero, A. (2022). Heuristic recommendation technique in Internet of Things featuring swarm intelligence approach. In Expert Systems with Applications (Vol. 187, p. 115904). Elsevier BV. https://doi.org/10.1016/j.eswa.2021.115904
48. Abualigah, Laith & Elsayed Abd Elaziz, Mohamed & Khodadadi, Nima & Forestiero, Agostino & Jia, Heming &Gandomi, Amir. (2022). Aquila Optimizer Based PSO Swarm Intelligence for IoT Task Scheduling Application in Cloud Computing. 10.1007/978-3-030-99079-4_19.
49. Abdelghani Dahou, Mohamed Abd Elaziz, Samia Allaoua Chelloug, Mohammed A.

Awadallah, Mohammed Azmi Al-Betar, Mohammed A. A. Al-qaness, Agostino Forestiero, "Intrusion Detection System for IoT Based on Deep Learning and Modified Reptile Search Algorithm", *Computational Intelligence and Neuroscience*, vol. 2022, Article ID 6473507, 15 pages, 2022. https://doi.org/10.1155/2022/6473507